

Structure-Based Design, Synthesis, and Biochemical and Pharmacological Characterization of Novel Salvinorin A Analogs as Active State Probes of the κ -Opioid Receptor[†]

Feng Yan,[‡] Ruslan V. Bikbulatov,^{||} Viorel Mocanu,^{§,▽} Nedyalka Dicheva,[§] Carol E. Parker,[§] William C. Wetsel,[⊥] Philip D. Mosier,[ⓐ] Richard B. Westkaemper,[ⓐ] John A. Allen,[‡] Jordan K. Zjawiony,^{||,#,‡} and Bryan L. Roth^{*,‡}

[‡]Department of Pharmacology and [§]UNC-Duke Proteomics Center, University of North Carolina, Chapel Hill, North Carolina 27599,
^{||}Department of Pharmacognosy, School of Pharmacy, University of Mississippi, University, Mississippi 38677, [⊥]Department of Cell

Biology, Duke University Medical Center, Durham, North Carolina 27710, [ⓐ]Department of Medicinal Chemistry, Virginia Commonwealth University, Richmond, Virginia 23298, [#]National Center for Natural Products Research, Research Institute of Pharmaceutical Sciences, School of Pharmacy, University of Mississippi, University, Mississippi 38677. [▽]Deceased.

Received April 8, 2009; Revised Manuscript Received June 17, 2009

ABSTRACT: Salvinorin A, the most potent naturally occurring hallucinogen, has attracted an increasing amount of attention since the κ -opioid receptor (KOR) was identified as its principal molecular target by us [Roth, B. L., et al. (2002) *Proc. Natl. Acad. Sci. U.S.A.* 99, 11934–11939]. Here we report the design, synthesis, and biochemical characterization of novel, irreversible, salvinorin A-derived ligands suitable as active state probes of the KOR. On the basis of prior substituted cysteine accessibility and molecular modeling studies, C315^{7,38} was chosen as a potential anchoring point for covalent labeling of salvinorin A-derived ligands. Automated docking of a series of potential covalently bound ligands suggested that either a haloacetate moiety or other similar electrophilic groups could irreversibly bind with C315^{7,38}. 22-Thiocyanatosalvinorin A (RB-64) and 22-chlorosalvinorin A (RB-48) were both found to be extraordinarily potent and selective KOR agonists in vitro and in vivo. As predicted on the basis of molecular modeling studies, RB-64 induced wash-resistant inhibition of binding with a strict requirement for a free cysteine in or near the binding pocket. Mass spectrometry (MS) studies utilizing synthetic KOR peptides and RB-64 supported the hypothesis that the anchoring residue was C315^{7,38} and suggested one biochemical mechanism for covalent binding. These studies provide direct evidence of the presence of a free cysteine in the agonist-bound state of the KOR and provide novel insights into the mechanism by which salvinorin A binds to and activates the KOR.

Salvinorin A, the active ingredient of the hallucinogenic plant *Salvia divinorum*, is the most potent known naturally occurring hallucinogen (1, 2). In 2002, we discovered that the κ -opioid receptor (KOR)¹ was the molecular target for the actions of salvinorin A in vitro (3). Studies with KOR knockout mice (4) unequivocally demonstrated that the KOR was also the site of action of salvinorin A in vivo, a finding which has been widely replicated (see refs 5 and 6 for reviews). Subsequently, salvinorin

A emerged as an attractive lead compound for drug discovery, and over the past few years, hundreds of salvinorin A derivatives have been synthesized (6). Some of these analogues present interesting pharmacological profiles, from full KOR agonist to partial δ -opioid receptor (DOR) or μ -opioid receptor (MOR) agonists and antagonists (7–11). However, most of the hundreds of analogues displayed decreased affinity (or even no affinity) for the KOR. The challenge now is to use the knowledge about salvinorin A–KOR interactions (12, 13) to design unique salvinorin A derivatives with novel pharmacological profiles and therapeutic potential. In recent years, covalently bound ligands emerged as a new class of receptor ligands with unique pharmacological properties. The successful design of the covalently bound ligands includes an allosteric modulator for the GABA_A receptor (14), fluorescently tagged inhibitors for calcium-bound protein arginine deiminase 4 (PAD4) (15), selective kinase inhibitors (16, 17), estradiols for the estrogen receptor (18, 19), and antagonists for the *N*-methyl-D-aspartate (NMDA) receptor (a ligand-gated cation channel) (20). This covalent labeling method takes advantage of the chemically reactive amino acids inside or close to the ligand binding site, and the reactive group is frequently a nucleophile. Because the recognition

[†]This research was supported in part by National Institutes of Health (NIH) Grant R01DA017204 (to B.L.R.) and the NIMH Psychoactive Drug Screening Program. J.A.A. was supported by a Neurodevelopmental Training Program Fellowship Grant from the NIH.

^{*}To whom correspondence should be addressed: Department of Pharmacology, 4072 Genetics Medicine Building, Medical School, University of North Carolina, Chapel Hill, NC 27599. Phone: (919) 966-7535. Fax: (919) 843-5788. E-mail: bryan_roth@med.unc.edu.

¹Abbreviations: GPCR, G protein-coupled receptor; KOR, κ -opioid receptor; hKOR, human KOR; Ga, G protein α subunit; TM, transmembrane domain; CHCA, α -cyano-4-hydroxycinnamic acid; CID, collision-induced dissociation; EL, extracellular loop; IL, intracellular loop; MALDI, matrix-assisted laser desorption ionization; MS, mass spectrometry; MS/MS, tandem mass spectrometry; *m/z*, mass-to-charge ratio; S/N, signal-to-noise ratio; TOF, time-of-flight; b_n and y_n, Bieman-modified Roepstorff and Fohlman peptide ion nomenclature.

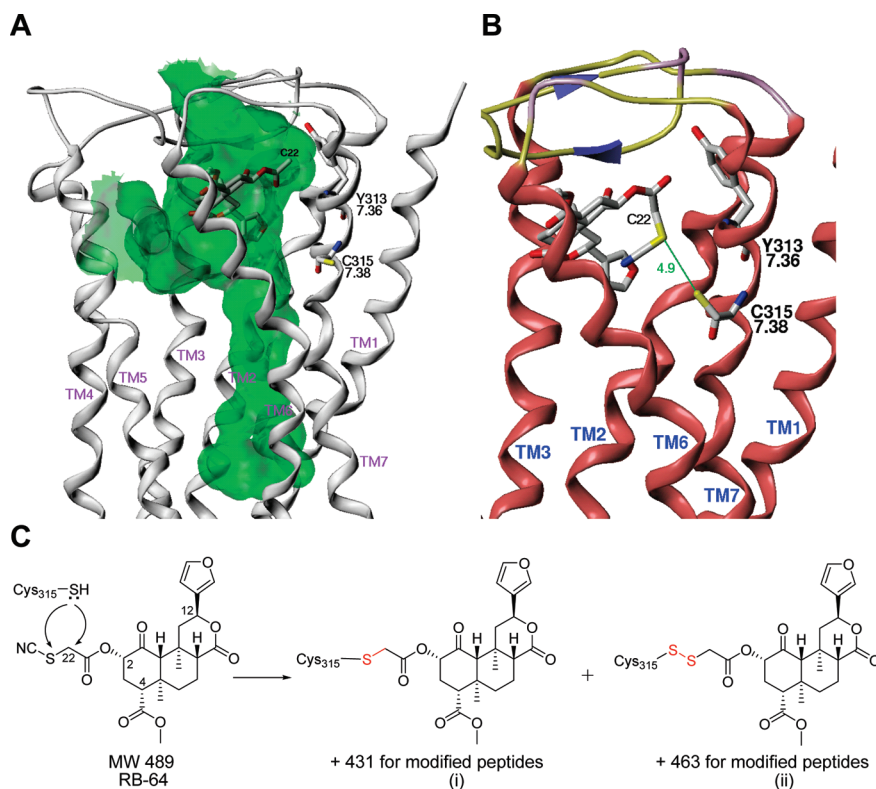


FIGURE 1: Molecular modeling reveals potential sites of adduct formation in the KOR. (A) The C-2 position of salvinorin A is in the proximity of Y313^{7,36} and C315^{7,38} in the wild-type (WT) KOR. Ribbons (white) indicate the position of the backbone, and a Connolly channel surface (green) describes the regions of steric accessibility within the activated receptor. An enlarged region of accessibility in the intracellular portion of the helical bundle is indicative of an activated GPCR. (B) The RB-64 thiocyanate group is in the proximity of C315^{7,38}. (C) The mechanisms for covalent labeling of cysteine involve nucleophilic substitution at C-22 or the adjacent S atom. The molecular weight change for the modified peptides is 431 (i) or 463 (ii) depending on the site of substitution.

between the ligand and receptor is specific, proximity-accelerated covalent labeling is expected to be highly selective. Introduction of a proper electrophilic group into the ligand structure is the key condition for promoting covalent labeling between the ligand and receptor. However, the structural variety of receptors and ligands creates uncertainty in choosing the optimal reactive group. Among the common reactive groups, halomethylketones, haloacetamides, isothiocyanates, Michael acceptors, aldol esters, nitrogen mustards, and other electrophilic moieties have been used for covalently bound ligands because of their relatively high reactivity under physiological conditions (e.g., pH 7.4).

Our prior molecular modeling studies predicted that a chemically reactive cysteine (C315^{7,38}) would reside in or near salvinorin A's binding site in the agonist-bound state of the KOR (12, 13, 21). Indeed, our prior studies showed there was a direct interaction between the acetoxy group of salvinorin A and Y313^{7,36}, a critical residue inside the binding pocket (12). Nearby, a water-accessible C315^{7,38} is highly reactive to methanethiosulfonate (MTS) reagent (Figure 1A), as reported in the substituted cysteine accessibility method (SCAM) studies by Xu et al. (22, 23) and us (21). Because the C315^{7,38}S mutation did not significantly affect salvinorin A's binding affinity, we predicted that C315^{7,38} exists as a free cysteine rather than as a contributor to disulfide bonds or the global structure of the KOR. Theoretically, C315^{7,38} could provide an anchoring point for covalent labeling.

In this paper, we describe molecular modeling studies which predict that 22-substituted salvinorin A derivatives will interact with C315^{7,38}. On the basis of these predictions, 22-thiocyanato-salvinorin A (RB-64) and 22-chlorosalvinorin A (RB-48) were synthesized and found to be extraordinarily potent, selective, and

apparently irreversible KOR agonists *in vitro*. *In vivo* studies revealed RB-64 to be 20-fold more efficacious than salvinorin A. Mutagenesis experiments and biochemical studies with purified KOR peptides *in vitro* confirmed the mechanism of irreversible binding to be nucleophilic substitution of C315^{7,38}. These studies provide convincing evidence for a free cysteine in or near the agonist-bound active state of the KOR.

EXPERIMENTAL PROCEDURES

Materials. Standard reagents were purchased from Sigma-Aldrich (St. Louis, MO). Some of the salvinorin A used as a standard in these studies was kindly provided by T. Prisinzano (University of Kansas, Lawrence, KS).

Syntheses and Characterization of 22-Chlorosalvinorin A (RB-48) and 22-Thiocyanatosalvinorin A (RB-64). Salvinorin B (25 mg, 64 μ mol) and catalytic (dimethylamino)-pyridine (DMAP) were dissolved in 5 mL of dichloromethane (DCM). Chloroacetyl chloride (10 mg, 90 μ mol) was added, and the reaction mixture was stirred at room temperature for 2 h. Then the solvents were evaporated in vacuo, and the residue was chromatographed on a silica gel (3:1 hexane/ethyl acetate) to yield 22-chlorosalvinorin A (22.7 mg, 76% yield): white solid; mp 216–218 °C; α_D^{20} −27.5 (*c* 0.08, MeCN); HRESIMS *m/z* [M + H]⁺ 467.1457 (calcd for C₂₃H₂₇ClO₈ 466.1394); ¹³C NMR (100 MHz, CDCl₃) δ 15.2, 16.4, 18.1, 30.5, 35.4, 38.1, 40.6, 42.1, 43.0, 51.2, 52.0, 53.3, 63.7, 71.9, 76.5, 108.5, 125.2, 139.6, 143.7, 166.6, 171.1, 171.4, 201.2; ¹H NMR (400 MHz, CDCl₃) δ 1.08 (s, 3H), 1.39 (s, 3H), 1.52–1.65 (m, 3H), 1.75 (m, 1H), 2.04–2.15 (m, 2H), 2.25–2.34 (m, 3H), 2.39 (dd, *J* = 5, 13 Hz, 1H), 2.76

Table 1: Pharmacological Profiles of Salvinorin Derivatives Substituted at C-22

	K_i^a (nM)	K_i^b (nM)	EC_{50}^c (nM)	relative E_{max} (%)
salvinorin A	1.8 ± 1.4	21 ± 11	17 ± 6	100
22-chlorosalvinorin A (RB-48)	2.1 ± 0.8 ^d	32 ± 15	0.19 ± 0.01	85 ± 3
22-thiocyanatosalvinorin A (RB-64)	0.59 ± 0.21	39 ± 11	0.077 ± 0.016	95 ± 2
22-bromosalvinorin A (RB-50)	1.5 ± 0.22	39.57 ± 11.56	11 ± 6	76 ± 7
(22 <i>R,S</i>)-22-chloro-22-methylsalvinorin A (RB-55)	21 ± 3	189 ± 70.12	35 ± 17	83 ± 10
(22 <i>S</i>)-22-chloro-22-methylsalvinorin A (RB-55-1)	30 ± 15	269 ± 48	160 ± 80	99 ± 12
(22 <i>R</i>)-22-chloro-22-methylsalvinorin A (RB-55-2)	58 ± 32	> 3000	273 ± 130	98 ± 8
22-methoxysalvinorin A (RB-65)	5.7 ± 1.2	431.3 ± 54.13	67 ± 22	99 ± 11
22,22-dichlorosalvinorin A (RB-66)	911 ± 170	> 10000	1678 ± 320	103 ± 14

^a The affinity constants (K_i) of the different compounds were determined in competition binding assays with [³H]U69593 and increasing concentrations of unlabeled compounds. Each value is the mean of three independent experiments. ^b The affinity constants (K_i) of the different compounds were determined in competition binding assays with [³H]diprenorphine. ^c The functional potencies (EC_{50}) of the different compounds were determined with an [³⁵S]GTP γ S assay. ^d RB-48 exhibited a two-site binding curve, which gave another higher affinity in the subpicomolar range.

(m, 1H), 3.70 (s, 3H), 4.18 (ABq, J = 15 Hz, 2H), 5.20 (m, 1H), 5.43 (dd, J = 5, 12 Hz, 1H), 6.36 (s, 1H), 7.37 (br s, 1H), 7.39 (s, 1H). 22-Chlorosalvinorin A (20 mg, 43 μ mol) was dissolved in anhydrous ethanol (2 mL) with potassium thiocyanate (5.4 mg, 56 μ mol). The reaction mixture was refluxed for 5 h, allowed to reach room temperature, and concentrated in vacuo. Water (2 mL) was then added, and the reaction mixture was extracted with chloroform (three 5 mL portions). Solvents were removed in vacuo, and the mixture was separated by HPLC [C₁₈ column, MeCN/H₂O (1:1), detection at 210 nm] to yield 22-thiocyanatosalvinorin A (16.6 mg, 79% yield): semisolid; α_D^{20} −32.5 (*c* 0.08, MeCN); HRESIMS m/z [M + H]⁺ 490.1519 (calcd for C₂₄H₂₇NO₈S 489.1452); IR (neat) 2160 cm^{−1} (SCN); ¹³C NMR (100 MHz, CDCl₃) δ 15.2, 16.4, 18.1, 30.5, 34.5, 35.5, 38.1, 42.1, 43.3, 51.3, 52.0, 53.3, 64.0, 71.9, 76.9, 108.4, 110.3, 125.2, 139.5, 143.8, 165.4, 170.9, 171.2, 200.6; ¹H NMR (400 MHz, CDCl₃) δ 1.13 (s, 3H), 1.45 (s, 3H), 1.58–1.68 (m, 3H), 1.82 (m, 1H), 2.08–2.24 (m, 3H), 2.33–2.41 (m, 2H), 2.48 (dd, J = 5, 13 Hz, 1H), 2.79 (m, 1H), 3.75 (s, 3H), 3.89 (s, 2H), 5.22 (m, 1H), 5.53 (dd, J = 5, 12 Hz, 1H), 6.40 (d, J = 1 Hz, 1H), 7.41 (m, 1H), 7.44 (s, 1H).

The other C-22-substituted salvinorin A derivatives (RB-50, RB-55, RB-55-1, RB-55-2, RB-65, and RB-66) presented in Table 1 were obtained in a manner analogous to that of RB-48 with the use of corresponding acyl chlorides.

(i) 22-Bromosalvinorin A (RB-50) was obtained in 55% yield using bromoacetyl chloride: brownish solid; mp 214–215 °C dec. RB-50 is a highly unstable at room temperature. It shows spectral features analogous to those of 22-chlorosalvinorin A (RB-48), but its instability makes the accurate spectral measurements practically impossible. To minimize decomposition, the products has to be stored in a deep-freezer prior to binding assays.

(ii) (22*R,S*)-22-Chloro-22-methylsalvinorin A (RB-55) was obtained in 83% yield using 2-chloropropionyl chloride: white solid; mp 198–200 °C; HRTOFMS m/z [M + H]⁺ 479.1464 (calcd for C₂₄H₂₈ClO₈ 479.1467); ¹³C NMR (100 MHz, CDCl₃) δ 15.2, 16.4, 18.1, 21.6, 30.6, 35.4, 38.1, 42.1, 43.3, 51.3, 52.0, 52.3, 53.4, 64.0, 72.0, 76.0, 108.4, 125.2, 139.5, 143.7, 169.1, 171.0, 171.4, 200.8; ¹H NMR (400 MHz, CDCl₃) δ 1.14 (s, 3H), 1.45 (s, 3H), 1.52–1.71 (m, 4H), 1.77 (d, J = 4.0 Hz, 3H), 1.78–1.83 (m, 2H), 2.08 (dd, J = 11.5, 2.8 Hz, 1H), 2.13–2.22 (m, 2H), 2.37 (dd, J = 13.6, 7.1 Hz, 2H), 2.51 (dd, J = 13.4, 5.1 Hz, 1H), 2.78 (m, 1H), 3.74 (s, 3H), 4.51 (ABq, J = 7.0 Hz, 1H), 5.17 (m, 1H), 5.52 (dd, J = 11.6, 5.1 Hz, 1H), 6.39 (s, 1H), 7.40 (br s, 1H), 7.42 (s, 1H).

RB-55 was chromatographically separated into individual 22S (RB-55-1) and 22R (RB-55-2) epimers. Both epimers had the same spectral characteristic features. The structure of the 22S

(RB-55-1) isomer was independently confirmed by X-ray crystallography.

(iii) 22-Methoxysalvinorin A (RB-65) was obtained in 79% yield using methoxyacetyl chloride: amorphous solid; HRTOFMS m/z [M + H]⁺ 461.1813 (calcd for C₂₄H₂₉O₉ 461.1806); ¹³C NMR (100 MHz, CDCl₃) δ 15.1, 16.3, 18.1, 30.6, 35.3, 37.9, 42.0, 42.9, 51.0, 51.9, 53.2, 59.3, 63.5, 69.3, 71.9, 75.2, 108.5, 125.2, 139.5, 143.6, 169.4, 171.2, 171.5, 201.6; ¹H NMR (400 MHz, CDCl₃) δ 1.03 (s, 3H), 1.36 (s, 3H), 1.48–1.61 (m, 3H), 1.69 (dd, J = 10.8, 8.0 Hz, 1H), 1.99–2.11 (m, 2H), 2.19–2.28 (m, 3H), 2.38 (dd, J = 13.5, 5.1 Hz, 1H), 2.73 (dd, J = 15.4, 7.4 Hz, 1H), 3.40 (s, 3H), 3.65 (s, 3H), 4.09 (ABq, J = 16.6 Hz, 2H), 5.19 (t, J = 10.0 Hz, 1H), 5.43 (dd, J = 11.7, 5.0 Hz, 1H), 6.32 (s, 1H), 7.33 (br s, 1H), 7.36 (s, 1H).

(iv) 22-Dichlorosalvinorin A (RB-66) was obtained in 86% yield using dichloroacetyl chloride: amorphous solid; ¹³C NMR (100 MHz, CDCl₃) δ 15.1, 16.4, 18.1, 30.3, 35.4, 38.1, 42.1, 42.9, 51.2, 52.0, 53.2, 63.8, 71.9, 76.7, 108.5, 109.3, 125.1, 139.6, 143.7, 163.8, 171.0, 171.2, 200.2; ¹H NMR (400 MHz, CDCl₃) δ 1.11 (s, 3H), 1.41 (s, 3H), 1.52–1.65 (m, 3H), 1.78 (dd, J = 10.2, 2.5 Hz, 1H), 2.04–2.15 (m, 2H), 2.27 (s, 1H), 2.33–2.45 (m, 3H), 2.78 (m, 1H), 3.72 (s, 3H), 5.20 (t, J = 10.0 Hz, 1H), 5.45 (dd, J = 11.7, 5.0 Hz, 1H), 6.07 (s, 1H), 6.38 (s, 1H), 7.39 (br s, 1H), 7.41 (s, 1H).

[³⁵S]GTP γ S Binding Assay. Ten different concentrations of testing compounds in appropriate concentrations were reached in binding buffer [50 mM Tris-HCl, 100 mM NaCl, 10 mM MgCl₂, and 1 mM EDTA (pH 7.4)]. The [³⁵S]GTP γ S assay was set up in 96-well sample plates (Wallac) designed for the 1450 MicroBeta Counter (PerkinElmer). Then 50 μ L of a drug solution, 50 μ L of [³⁵S]GTP γ S (PerkinElmer, 1250 Ci/mmol), and 50 μ L of membrane and 20 μ M guanosine 5'-diphosphate (GDP) were added to 96-well plates and incubated for 20 min at room temperature, and then 50 μ L of beads (FlashBlue, PerkinElmer, 100 mg/mL stock, 110 μ L of stock solution/plate) was added to the mixture. The plates were shaken for 0.5 h on a titer plate shaker (Lab-line Instruments, Inc.), spun down at 1000 rpm (~270g) for 2 min, and counted using an ³⁵S protocol with a 1450 MircoBeta Counter (PerkinElmer).

Transient and Stable Expression of the KOR. HEK293 T cells were grown in 15 cm culture dishes in medium with 10% FBS in a humidified atmosphere consisting of 5% CO₂ at 37 °C. The confluent cells were transfected with wild-type (WT) KOR-peDNA3.1(+) FLAG-KOR-His₆ (25 μ g/15 cm dish), using Fugene 6 transfection reagent (Roche). It contains an N-terminal FLAG tag and a C-terminal His₆ tag. Another Flp-in CHO cell

line (Invitrogen), stably expressing the hKOR without any epitope tag, was used for studying the washing-resistant RB-64 labeling. The expression of KOR in these cells had been characterized by various radioligand binding and Western blotting assays. The affinity constants (K_i) of the different compounds were determined in competition binding assays with [3 H]U69593 and [3 H]diprenorphine. The details have been described in our previous reports (12, 13).

Labeling of Synthetic KOR Peptides. Synthetic peptides were custom prepared by the Tufts University Core Facility and incubated (1 mg/mL) together with RB-64 overnight at 37 °C in PBS; peptides were then prepared for MS as previously detailed (24).

Irreversible Binding Studies. After transfection for a total of 48 h, cell medium was removed and the transfected cells were washed with cold PBS; then the cells were labeled with RB-64 or RB-48 for various periods of time (5 min to several hours) and at various concentrations (from 0.1 nM to 30 μM) in ice-cold PBS. Cells were detached and centrifuged. Cell pellets were then extensively washed with standard binding buffer, centrifuged at 15000g for 20 min at 4 °C, and prepared for subsequent radioligand binding.

Mass Spectrometric Analysis. MS and MS/MS studies on the labeled synthetic peptide (Tufts University Core Facility) were performed on an Applied Biosystems 4800 Proteomics Analyzer (MALDI-TOF/TOF), using CHCA as the matrix.

Prepulse Inhibition Animal Study. Adult naive male and female C57BL/6J mice (Jackson Laboratories, Bar Harbor, ME) were used in all experiments. Animals were maintained under a 14 h–10 h light–dark cycle in a humidity- and temperature-controlled room with water and laboratory chow supplied. All experiments were conducted in accordance with NIH guidelines and under an approved protocol from the Institutional Animal Care and Use Committee at Duke University and the University of North Carolina.

Salvinorin A and RB-64 Disrupt Prepulse Inhibition (PPI) in C57BL/6J Mice. Mice were treated with vehicle [1% Tween 80 in Milli-Q water; 8 mL/kg, intraperitoneally (ip)] or one of four doses of salvinorin A (0.25, 0.5, 1.0, or 2.0 mg/kg, ip) or RB-64 (0.005, 0.01, 0.05, or 0.1 mg/kg, ip) immediately before being placed into the PPI apparatus (Med-Associates). In antagonist control studies, mice were treated with 10 mg of norbinaltorphimine (Nor-BNI)/kg ip, a long-acting selective KOR antagonist, 24 h prior to administration of 2.0 mg of salvinorin A/kg or 0.1 mg of RB-64/kg ($n = 6$). After being acclimatized to 62 dB white noise for 5 min, animals were subjected to 84 test trials, beginning and ending with 10 trials each of startle-only stimuli (40 ms, 120 dB white noise burst). The 64 remaining trials were randomized between the following trial types: eight startle-only trials, eight trials without any stimuli (null trials), 16 trials with prepulse stimuli (4, 8, 12, and 16 dB above the 62 dB background, four of each intensity, 20 ms in length) that were not paired with startle stimuli (prepulse-only trials), and 32 trials of prepulse stimuli (4, 8, 12, and 16 dB above the 62 dB background, eight at each intensity) paired with the 120 dB startle stimulus given 100 ms following the onset of the prepulse stimulus. Trials were separated by a variable interval (8–15 ms), and the total test time was 26–30 min for each animal. The data were analyzed with SPSS 11 programs (SPSS Inc.) and are presented as means ± the standard error of the mean. Differences in treatment effects on null activity, baseline startle responses, and overall PPI were analyzed with ANOVA, with the main effects of dose nested

within compound. Repeated measures ANOVA (RMANOVA) was used to examine the effects of salvinorin A and RB-64 on prepulse-dependent PPI, with prepulse intensity (4, 8, 12, and 16 dB) as the within subjects effect, and compound and dose as the between subjects effects (dose nested within compound). Differences between treatment groups were determined with Bonferroni corrected pairwise comparisons. In all cases, a p of < 0.05 was considered statistically significant.

Molecular Modeling. Unless otherwise noted, all molecular modeling procedures were conducted using SYBYL 8.1 (Tripos, LP, St. Louis, MO) on an Irix-based SGI Tezro, a SuSE Linux Enterprise Server-based SGI VSS40, or a Red Hat Enterprise Linux-based Hewlett-Packard xw9400 workstation. The Balles-ters–Weinstein amino acid residue numbering system (25) is used to identify conserved residue positions within the TM helices and is given as a superscript following the amino acid identifier, e.g., C315^{7,38}.

The construction and refinement of the KOR–salvinorin A interaction model have been previously described (12, 13, 21). The docked RB-64–KOR complex was obtained by modifying the C-22 position of salvinorin A with a thiocyanate group followed by an energy minimization procedure (Tripos Force Field; Gasteiger-Huckel charges; distance-dependent dielectric constant $\epsilon = 4.0$; termination criterion: energy gradient of < 0.05 kcal mol⁻¹ Å⁻¹). The +431 and +463 salvinorin A-labeled KOR models were constructed by manually joining the docked salvinorin A C-22 atom to the KOR C315^{7,38} S' sulfur atom with the appropriate linker, as these moieties were in the proximity of one another (Figure 1B). This was followed by energy minimization as described above. The +431 and +463 salvinorin A-labeled F314^{7,37}C/C315^{7,38}S KOR mutant models were obtained by mutating F314^{7,37} and C315^{7,38} to cysteine and serine, respectively. This was followed by a clockwise rotation (when viewed from the extracellular side) of residues L309^{7,32}–A317^{7,40} by 100° to position C314^{7,37} in the region of space previously occupied by C315^{7,38}. The interfacial regions between the rotated TM7 segment and the unrotated parent KOR structure (T302^{EL3}–L309^{7,32} and A317^{7,40}–S323^{7,46}) were then remodeled using loop searches. This was followed by repositioning of the side chains in the rotated segment using SCWRL 3.0 (26). Finally, the ligand was covalently bound to C314^{7,37} as described above for the WT KOR and energy-minimized. The stereochemical quality of the models was assessed using PRO-CHECK (27) and the ProTable facility within SYBYL to verify that the modifications did not abnormally distort the receptor structure.

RESULTS

Design and Synthesis of Extraordinarily Potent, Selective, and Potentially Irreversible Ligands for the κ -Opioid Receptor. Our previously reported (21) activated KOR–salvinorin A model (Figure 1A) showed C315^{7,38} to be accessible from within the binding pocket and relatively close to the C-2 acetyl group of salvinorin A. In this model, the C-2 acetyl group (C-22 atom) engages in van der Waals interactions with the aromatic side chain of Y313^{7,36}, an interaction that has been suggested (12, 13) to be an important contributor to the unusually high binding affinity and efficacy of salvinorin A. By modifying the conformation of the C-2 acetyl group and switching the C315^{7,38} side chain rotameric state from *gauche*– to *gauche*+, we may bring the C-22 and C315^{7,38} S' atoms within 5 Å of one another (Figure 1B).

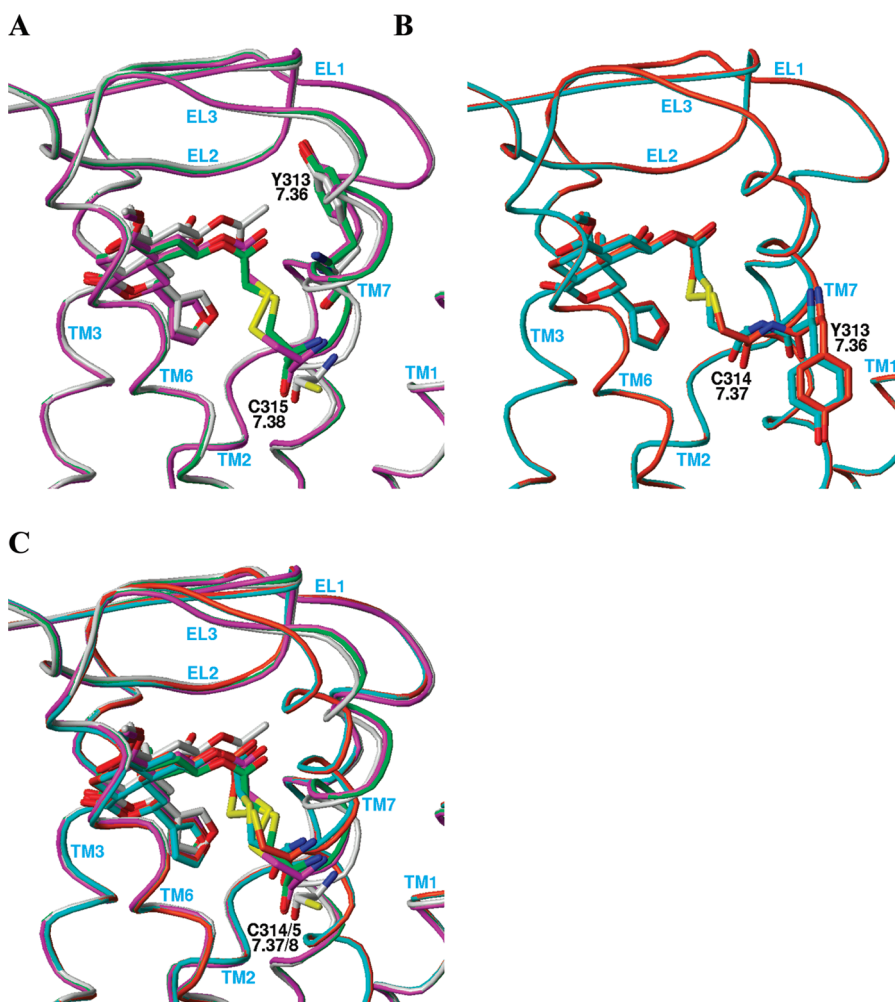


FIGURE 2: Comparison of the binding modes of salvinorin A and the +431 and +463 adducts. The colors of the backbone ribbons and displayed carbon atoms identify the receptor–ligand complex. (A) WT KOR: salvinorin A (white), +431 adduct (green), and +463 adduct (magenta). (B) F314^{7,37}C/C315^{7,38}S KOR double mutant: +431 adduct (cyan) and +463 adduct (orange). (C) All receptor–ligand complexes displayed in the same frame of reference. See the text for details.

This arrangement also allows a small substituent at C-22; the electrophilic thiocyanate derivative RB-64 is shown in Figure 1B.

Experimental evidence obtained using the substituted cysteine accessibility method (SCAM) by Xu et al. (22, 28) and us (21) suggests that there is significant rotational flexibility in the extracellular regions of both TM6 and TM7 about their helical axes. Helical rotations are also thought to be important for GPCR activation (see ref 29 for a current review) and are most likely a property of transmembrane helices in general, especially those containing proline (30) and/or glycine (31). This rotational flexibility should facilitate nucleophilic attack by the C315^{7,38} thiol at either C-22 or an adjacent electrophilic site without requiring significant reorientation of the ligand. For RB-64, the resulting labeled KOR receptor models result in either a thioether (+431 label; substitution of a thiocyanato group) or a disulfide (+463 label; substitution of a cyano group) linkage as shown in Figure 1C.

Modeling of the +431- and +463-labeled WT KOR resulted in ligand–receptor complexes whose conformation was minimally perturbed compared to that of the unlabeled salvinorin A–KOR complex (Figure 2A,B.) The change in position of the salvinorin A heavy atoms (not including the C-2 substituent) was 0.63 Å for the +431 label and 0.52 Å for the +463 label (Figure 2A). A similarly small displacement of the KOR backbone in the

region of C315^{7,38} was also noted. These results suggest that salvinorin A analogues substituted with electrophilic groups at C-22 would be effective and selective affinity labels for the KOR. On the basis of these considerations, several salvinorin A derivatives substituted at the C-22 position were synthesized and pharmacologically characterized. Of these, several emerged as potent KOR ligands (Table 1) with the agonist 22-thiocyanatosalvinorin A (RB-64) demonstrating the highest affinity (0.59 nM). 22-Thiocyanatosalvinorin A also emerged as a subnanomolar efficacy agonist in [³⁵S]GTPyS binding assays. To the best of our knowledge, RB-64 represents the most potent KOR agonist thus far identified. No significant activity (K_i values of ≥ 10000 nM) at μ - or δ -opioid receptors was revealed for these compounds (not shown).

22-Thiocyanatosalvinorin A Wash-Resistant Irreversible Binding and Mutagenesis Studies of the KOR. Because 22-thiocyanatosalvinorin A and 22-chlorosalvinorin A were predicted to be irreversible inhibitors on the basis of molecular modeling considerations, we next determined if prolonged incubations with either compound led to washing-resistant inhibition of binding. In preliminary studies, we found incubation at 4 °C with either 22-thiocyanatosalvinorin A or chlorosalvinorin A resulted in wash-resistant inhibition of binding but that 22-thiocyanatosalvinorin A's was more robust (not shown).

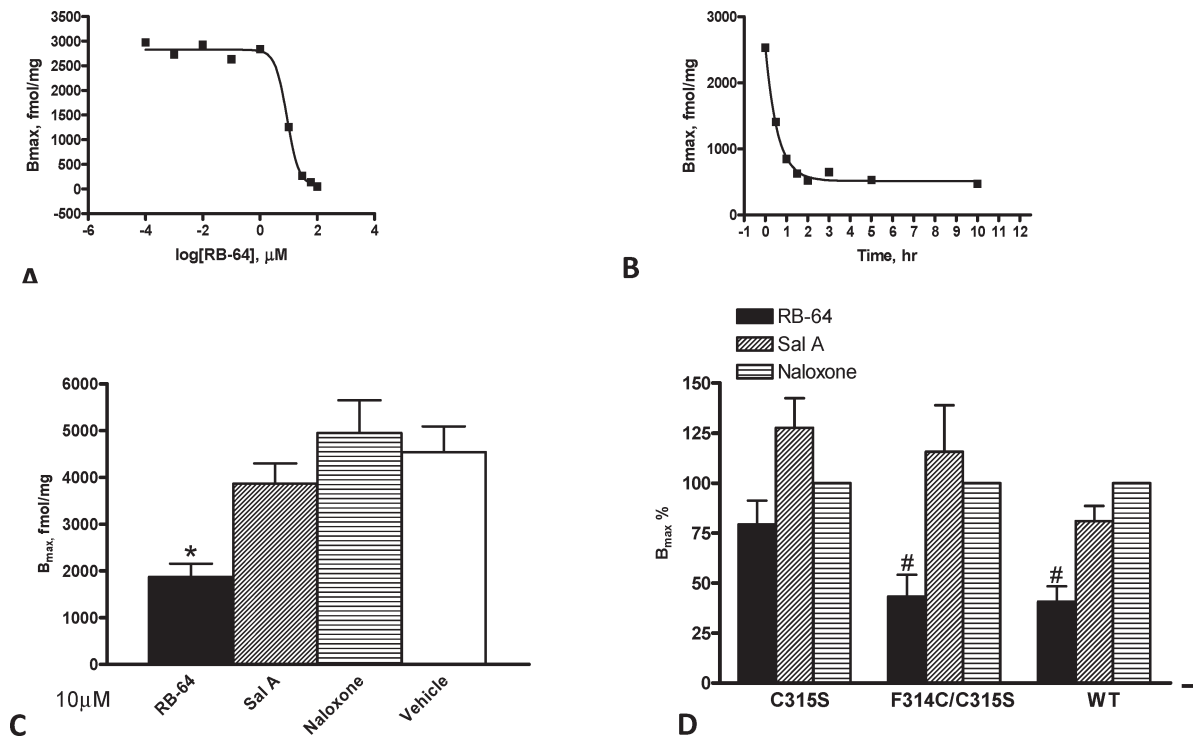


FIGURE 3: RB-64 induces wash-resistant inhibition of KOR binding at C315. (A) Dose-response curve for RB-64 for wash-resistant inhibition of binding at 4 °C (2 h) yielding an EC₅₀ of 1.2 μM . (B) Time course study at 4 °C with a maximally effective dose of RB-64 (10 μM) yielding a t_{1/2} of 0.4 h. (C) Cells expressing the KOR were exposed at 10 μM for 3 h to RB-64, salvinorin A, naloxone, and vehicle (DMSO only). After incubation, the cell membranes were extensively washed (at least three times); the residual binding was determined by [³H]diprenorphine saturation binding. Data presented are B_{\max} values for two to four independent experiments. (D) B_{\max} values of various mutants after they had been labeled with RB-64, salvinorin A, and naloxone. B_{\max} values are expressed as a percentage of vehicle control. Each bar represents the mean \pm standard error of the mean for two to four independent experiments. An asterisk indicates that RB-64 labeling was significantly different ($p < 0.01$) from the reference (vehicle) by ANOVA. A number sign indicates that RB-64 labeling was significantly different ($p < 0.05$) from that of naloxone by ANOVA.

A time course and dose-response study of 22-thiocyanatosalvinorin A disclosed a t_{1/2} of 0.4 h and an EC₅₀ of 9 μM for wash-resistant inhibition of binding (Figure 3A,3B) at 4 °C. Under these conditions, radioligand binding was weakened, although there was no change in total KOR protein as assessed by Western blot analysis (not shown). For further experiments, the conditions (3 h and 10 μM at 4 °C in PBS buffer) that gave highly reproducible wash-resistant inhibition of binding were chosen. Under these conditions, a maximum of 59% of the KOR could be labeled by 22-thiocyanatosalvinorin A (Figure 3C). For controls, identical incubations with either salvinorin A or naloxone did not substantially alter radioligand binding. Longer incubation times with higher concentrations of 22-thiocyanatosalvinorin A (e.g., 10 h and 20 μM) achieved 82% wash-resistant inhibition of KOR binding (not shown). Other high-affinity ligands (e.g., 22-bromo-salvinorin A) were also tested as potential affinity ligands, although none exhibited significant irreversible inhibition of binding.

As indicated previously, molecular modeling studies predicted that 22-thiocyanatosalvinorin A would interact with C315^{7,38}. Accordingly, the C315^{7,38}S single and F314^{7,37}C/C315^{7,38}S double mutants were tested for wash-resistant inhibition of binding (Figure 3D). As expected, C315^{7,38}S did not exhibit any apparent reactivity with 22-thiocyanatosalvinorin A as compared to naloxone. Significantly, F314^{7,37}C/C315^{7,38}S, which is predicted to introduce a free thiol in the vicinity of the thiocyanato group, produced significant apparent reactivity.

In the WT KOR–salvinorin A complex (Figure 1A), the F314^{7,37} side chain is oriented away from the binding pocket. However, the putative rotational flexibility of the extracellular

region of TM7 mentioned above allows position 7.37 to be accessed by a ligand from within the binding cavity. In many of the experimentally determined GPCR structures published to date, TM7 contains an “overwound” section of 3₁₀-helix at positions 7.41–7.46 followed by a conserved proline-induced kink at positions 7.46–7.48. Residues on TM7 following position 7.48 (in the intracellular region) are involved in an H-bonding network (“NPXXY”) that is highly conserved among rhodopsin-like GPCRs. Thus, one possible explanation for the observed pattern of enhanced accessibility (21) of the residues in the TM7 extracellular region is that this overwound section can become “unwound”, resulting in an α - or π -helical geometry and a corresponding clockwise rotation of the extracellular portion of TM7 (as viewed from the extracellular side). The amount of rotation needed to make position 7.37 ligand-accessible is roughly 100° (3.6 residues per turn in a regular α -helix = 100° per residue), which will introduce a bulge similar to the conserved π -bulge observed in TM5 of rhodopsin-like GPCRs (32). Such “wide turn” regions are known to impart flexibility to transmembrane-spanning helices (33). In the KOR, the overwound region also contains a glycine residue, G319^{7,42}, that will tend to increase the local flexibility of the backbone because of the absence of a side chain and further promote the rotation of the extracellular region of TM7. RB64-labeled F314^{7,37}C/C315^{7,38}S double mutant KOR models were generated with these concepts in mind and are shown in panels B and C of Figure 2.

Identification of a Potential Mechanism for Irreversible Inhibition of Binding Using Model Peptide Substrates. Covalently bound ligands can label the cysteine residue through different chemical pathways. To explore the possible reaction

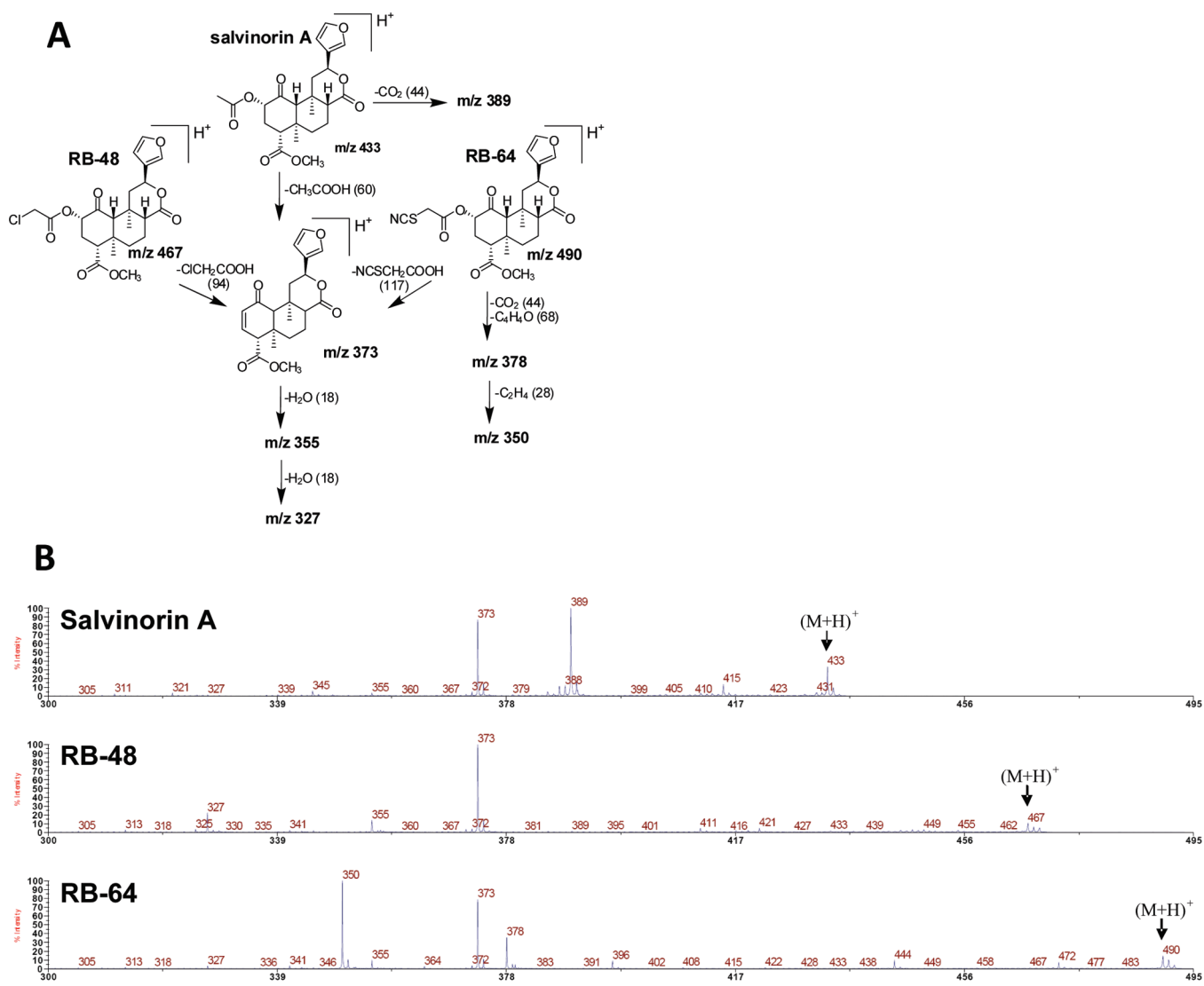


FIGURE 4: Fragmentation pathways for salvinorin A, RB-48, and RB-64. (A) Deduced structures of the major identified fragments. (B) MS/MS spectra for salvinorin A, RB-48, and RB-64 (from top to bottom), whose precursor ions are at m/z 433, 467, and 490, respectively.

pathways, a synthetic model peptide (Ac-YFCIALGY) was used to mimic the covalent labeling between RB-64 and the KOR protein. A parallel mass spectrometric examination of RB-64, RB-48, and salvinorin A revealed the possible fragmentation mechanisms of the parent compounds (Figure 4A,B). All of the major product ions were assigned, including m/z 378, 373, 355, and 350, and our control observations for salvinorin A are in excellent agreement with prior studies (34, 35) while the results with RB-64 and RB-48 are new.

After incubation of RB-64 with the model peptide at 37 °C overnight, one major product (m/z 1475) was identified via MS (Figure 5B). This indicated that free peptide labeling preferred nucleophilic substitution of the cyano group with the formation of a disulfide bond as shown in Figure 1C. This new pathway was confirmed by the MS/MS analysis of m/z 1475 (Figure 5C).

22-Thiocyanatosalvinorin A Is Extraordinarily Potent in Vivo. Prepulse inhibition (PPI) is a measure of sensory motor gating (36–38), and a large number of studies have validated disruption of PPI as an indicator of potential psychotomimetic properties. Because salvinorin A is the most potent naturally occurring hallucinogen (5), we predicted that both 22-thiocyanatosalvinorin A and salvinorin A have effects on PPI. We

observed an extraordinarily high potency of RB-64 as compared to that of salvinorin A. Salvinorin A and RB-64 produced changes in activity during null trials (without any stimuli) compared to vehicle-treated mice (Table 2). Mice treated with salvinorin A showed significant increases in null activity with 0.5 mg/kg ($p < 0.001$) compared to all other doses of the compound and vehicle controls. Effects of RB-64 were somewhat different. The two smaller doses of RB-64 had little effect on null activity, whereas the two largest doses resulted in increased activity compared to the vehicle control ($p < 0.001$).

Mice treated with salvinorin A or RB-64 showed dose-dependent parabolic changes in baseline startle activity (Figure 6A). Overall PPI was affected by salvinorin A (Figure 6B) and 22-thiocyanatosalvinorin A (Figure 6C). Bonferroni corrected pairwise comparisons found that overall inhibition was similar for vehicle and 0.25, 0.5, or 1 mg of salvinorin A/kg, while 2 mg/kg significantly suppressed inhibition ($p < 0.044$). By comparison, RB-64 at 0.01 and 0.05 mg/kg resulted in marked increases in the overall level of inhibition compared to the vehicle control ($p < 0.021$). Mice given 0.1 mg of RB-64/kg showed a significant reduction in the overall level of inhibition relative to vehicle-treated mice ($p < 0.046$). Mice treated with vehicle showed

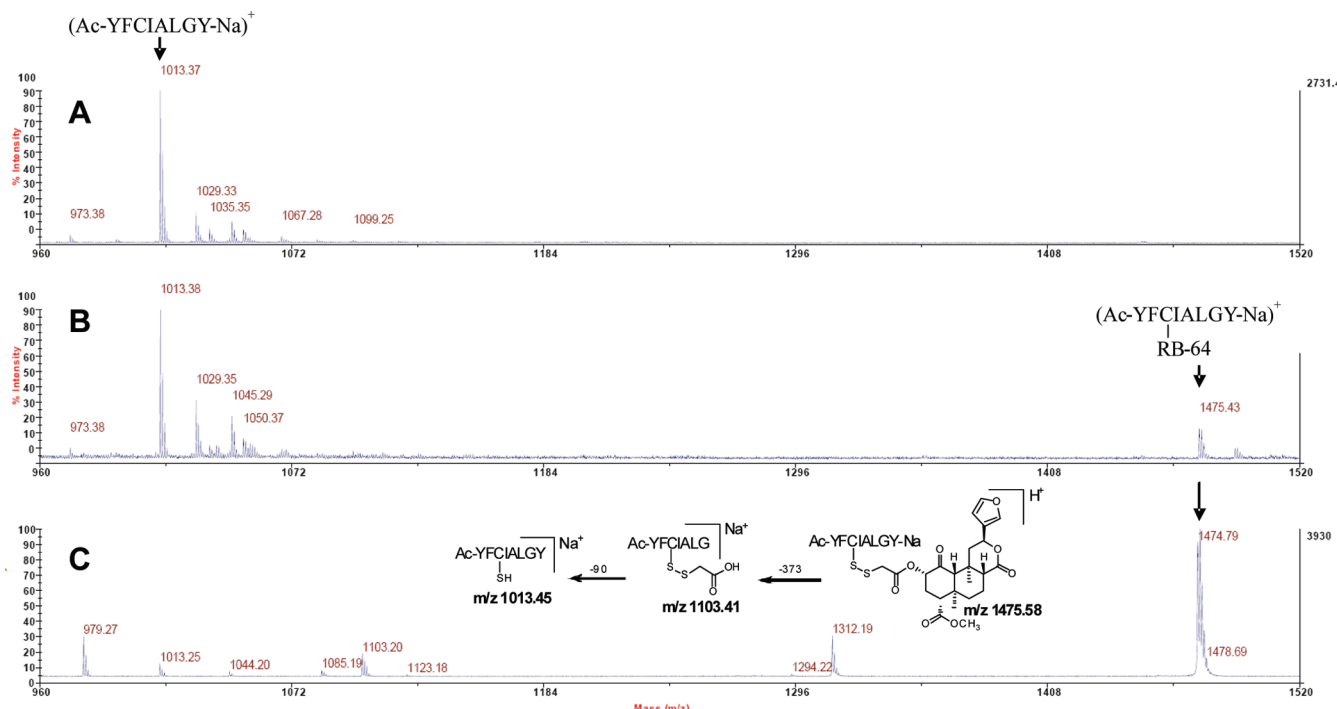


FIGURE 5: Identification of the adduct at C315 via model KOR peptides. MS spectra of unlabeled (A) and RB-64-labeled (B) peptide Ac-YFCIALGY-Na and MS/MS spectrum with m/z 1475.5 (C), which contains several major fragments from the RB-64-modified peptide.

Table 2: Null Activity Levels in Mice Treated with Vehicle, Salvinorin A, or RB-64

treatment	null activity (mA displacement)
10% Tween vehicle	11.16 ± 4.34
salvinorin A	
0.25 mg/kg	19.44 ± 5.83
0.5 mg/kg	28.79 ± 3.99 ^a
1.0 mg/kg	13.63 ± 3.65
2.0 mg/kg	13.76 ± 3.65
RB-64	
0.005 mg/kg	8.22 ± 3.73
0.01 mg/kg	16.81 ± 4.4
0.05 mg/kg	64.89 ± 10.88 ^a
0.1 mg/kg	51.6 ± 12.16 ^a

^a $p < 0.05$ compared to vehicle controls.

prepulse-dependent PPI. Salvinorin A or RB-64 disrupted prepulse-dependent PPI at all prepulse intensities. Mice given 0.25, 0.5, or 1 mg of salvinorin A/kg had increased PPI to the 4 dB prepulse, relative to vehicle ($p < 0.05$) (Figure 6B); PPI responses at the 8 and 12 dB prepulses were similar for animals treated with vehicle or 0.25, 0.5, or 1 mg of salvinorin A/kg. However, mice given 2 mg of salvinorin A/kg had marked reductions in PPI at the 8, 12, and 16 dB prepulses compared to vehicle ($p > 0.011$) or all other doses of the compound ($p < 0.047$); responses to 4 dB were unchanged from the vehicle control. When animals were given 0.005, 0.01, or 0.05 mg of RB-64/kg, PPI to the 4 dB prepulse was enhanced relative to vehicle ($p < 0.047$) (Figure 6C). By comparison, 0.005 mg RB-64 depressed responses to the 12 and 16 dB prepulses ($p < 0.010$). The 0.01 and 0.05 mg/kg doses increased PPI to the 8 dB prepulse relative to the vehicle controls ($p < 0.031$). Similarly, 0.05 mg of RB-64/kg strengthened the responses to the 12 and 16 dB prepulses ($p < 0.052$). Responses to the largest doses of RB-64 were different from those for the 0.01 and 0.05 mg/kg doses. Here, responses to the 12 and 16 dB

prepulses were significantly depressed compared to the vehicle control ($p < 0.003$). In antagonist control studies, mice were treated with the selective KOR antagonist *nor*-binaltorphimine (Nor-BNI) (10 mg/kg) prior to administration of 2.0 mg of salvinorin A/kg or 0.1 mg of RB-64/kg (Figure 6D,E). Nor-BNI antagonized salvinorin A and RB-64-induced disruption of PPI, indicating the behavioral responses of both compounds are mediated by KOR.

DISCUSSION

In this paper, we report the successful modeling-based design, synthesis, and pharmacological characterization of novel salvinorin A-derived KOR affinity ligands. Diffusible ligands bind to receptors mainly through noncovalent interactions, such as electrostatic forces, hydrogen bonds, van der Waals forces, and hydrophobic effects. In contrast, affinity ligands can directly link to the receptor protein and thus can present with unique biophysical and pharmacological properties. As is evident, RB-64 displays high affinity, potency, and selectivity for the KOR (Table 1), and this indicates that affinity ligands can significantly improve the efficacy and selectivity for their corresponding receptors without the introduction of off-target effects. As an apparent affinity ligand, RB-64 shows great potential as a molecular probe for exploring κ -opioid receptor structure and function. To the best of our knowledge, RB-64 represents the first selective agonist affinity ligand for KORs. These studies also provide the first direct evidence of a reactive cysteine in the binding pocket of the KOR in support of many prior modeling and biochemical studies.

On the basis of our previous binding site model (12, 13, 21), the C-2 position of salvinorin A is in the proximity of Y313^{7,38}, so that residues C315^{7,36} and F314^{7,37} are in a favorable position for covalent labeling. Our rational design of affinity ligands based on the structure of salvinorin A further confirmed the proposed binding mode interaction between the KOR and salvinorin A.

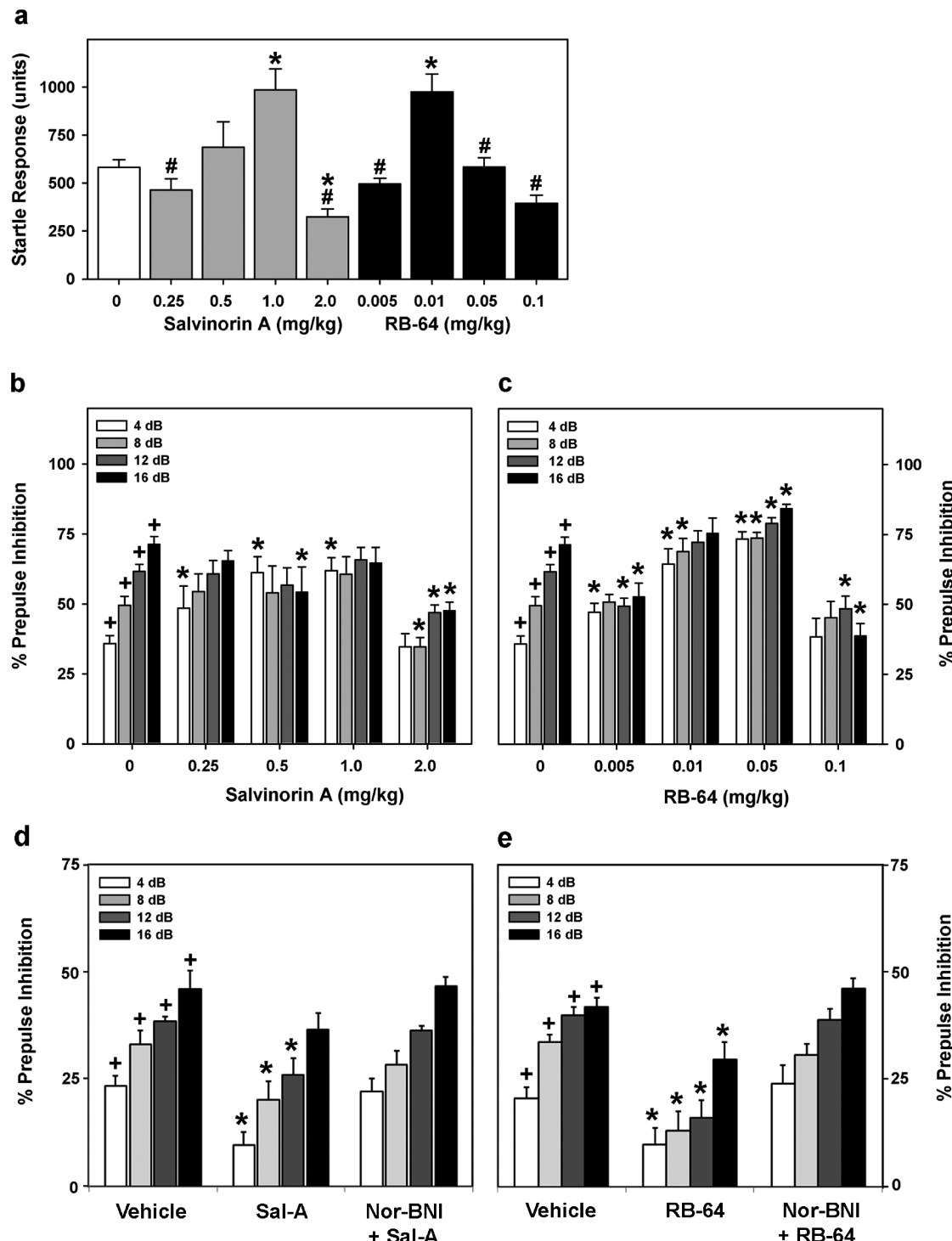


FIGURE 6: RB-64 is a potent psychotomimetic agent in vivo. (A) Startle responses to the 120 dB stimulus for animals treated with different doses of salvinorin A or RB-64. A number sign indicates $p < 0.05$ in comparisons of startle responses to 0.5 mg of salvinorin A/kg or 0.01 mg of RB-64/kg. (B) Percent PPI to the 4, 8, 12, and 16 dB prepulses for animals given various doses of salvinorin A. (C) Percent PPI to the 4, 8, 12, and 16 dB prepulses for animals given various doses of RB-64 ($N = 10\text{--}16$ mice per treatment). (D) Percent PPI to the 4, 8, 12, and 16 dB prepulses for animals treated with 2 mg of salvinorin A/kg or 10 mg of Nor-BNI/kg followed by 2 mg of salvinorin A/kg ($N = 6$ mice per treatment). (E) Percent PPI to the 4, 8, 12, and 16 dB prepulses for animals treated with 0.1 mg of RB-64/kg or 10 mg of Nor-BNI/kg followed by 0.1 mg of RB-64/kg ($N = 6$ mice per treatment). An asterisk indicates $p < 0.05$ compared to vehicle controls; a plus sign indicates $p < 0.05$ in comparisons of prepulse-dependent PPI at the 4, 8, 12, and 16 dB prepulses within a single treatment.

Interestingly, in the labeling experiment, RB-64 can undergo two different chemical reaction pathways (Figure 1C). In a restricted biological environment, such as the binding pocket of KOR, multiple factors (e.g., ligand orientation, space restriction, etc.) will not allow all of the possible chemical reactions to occur. Indeed, the mass spectrometric analysis of the short synthetic

peptide (YFCIALGY) revealed a substitution of the cyano group, and in future studies, it will be important to determine if this reaction mode is conserved in the intact KOR.

These studies are significant because they clearly demonstrate that the modeling-based synthesis of affinity ligands can be highly successful. Our ability to predict the orientation and mode of

binding of the various salvinorin A derivatives we prepared was highly dependent on prior studies in which we applied a variety of approaches, including molecular modeling, directed mutagenesis, substituted cysteine-accessibility mutagenesis, and salvinorin A analogue synthesis to arrive at a testable model of binding of agonist to the KOR.

Our synthetic design of salvinorin A-derived irreversible affinity labels assumed the introduction of electron-withdrawing groups at C-22 to increase the electrophilicity of this center and make it capable of forming a covalent bond with the SH group of C315. We selected halogen atoms (e.g., chlorine and bromine) for this purpose because of their good leaving group character for nucleophilic substitution with thiols. Several salvinorin A derivatives having one or two chlorine atoms at C-22 were synthesized (see Table 1). In this group of compounds, 22-bromo- and 22-chlorosalvinorin (RB-48) were comparable to salvinorin A in KOR binding affinity. Interestingly, replacement of the chlorine atom with an electron-donating methoxy group only slightly lowered the affinity. Finally, introduction of a thiocyanate group via a simple reaction with potassium thiocyanate afforded us a ligand which apparently covalently bound to the KOR and activated the receptor with exceptionally high potency. The difference between the binding affinity at room temperature with purified membranes (39 nM at the [^3H]diprenorphine-labeled KOR) and the EC₅₀ for apparent irreversible labeling in intact cells (1200 nM) is commonly seen with affinity ligands and has been previously reported with opioid affinity ligands (39–42).

The thiocyanate group is not commonly used in affinity labeling. Indeed, only a few futile attempts of using this group are known. Much more commonly used isothiocyanates provided good labels in the formation of covalent bonds with free amino group of proteins in addition rather than substitution reactions. Reactions of isothiocyanates with cysteine residues, although known, are much less common. Another advantage of thiocyanato derivatives over isothiocyanates is the simplicity of the synthesis from corresponding chloro derivatives. 22-Thiocyanatosalvinorin (RB-64) is a solid and stable compound and may be stored for a prolonged period of time without decomposition. Finally, it is evident that thiocyanatosalvinorin (RB-64) is considerably more potent than salvinorin A at disrupting sensory motor gating in vivo, and these results are in good agreement with its enhanced agonist potency in vitro.

In conclusion, we describe the first successful model-based design and synthesis of agonist affinity ligands for the KOR–thiocyanatosalvinorin (RB-64) complex. We also provide a reasonable model describing RB-64's mode of interaction with KOR via mutagenesis studies and high-resolution proteomics studies of model KOR membrane protein synthetic peptides. These studies provide the first direct evidence of the presence of a free cysteine in the agonist-bound state of the KOR and provide novel insights into the mechanism by which salvinorin A and its analogues bind to and activate the KOR.

ACKNOWLEDGMENT

We thank Drs. Vernon E. Anderson, Martin D. Snider, Paul R. Ernsberger, and Krzysztof Palczewski for comments and suggestions on the manuscript. The pcDNA3.1(+) FLAG-KOR-His₆ vector was made by Dr. Timothy A. Vortherms. The Flp-In CHO cell line (Invitrogen) stably expressing the hKOR was made by Joe Rittiner. J.K.Z. thanks Lukasz Kutrzeba for his help with NMR measurements. Mass spectro-

meters were provided by both the Department of Pharmacology of the University of North Carolina and the UNC-Duke Proteomics Center, which was partially funded by a gift from an anonymous donor. This paper is dedicated to the memory of Viorel Mocanu, PhD.

REFERENCES

- Ortega, A., Blount, J. F., and Manchand, P. S. (1982) Salvinorin: A new *trans*-neoclerodane diterpene from *Salvia divinorum* (Labiatae). *J. Chem. Soc., Perkins Trans. 1*, 2505–2508.
- Valdes, L. J., Butler, W. M., Hatfield, G. M., Paul, A. G., and Koreeda, M. (1984) Divinorin A: A psychotropic terpenoid and divinorin B from the hallucinogenic Mexican mint *Salvia divinorum*. *J. Org. Chem.* 49, 4716–4720.
- Roth, B. L., Baner, K., Westkaemper, R., Siebert, D., Rice, K. C., Steinberg, S., Ernsberger, P., and Rothman, R. B. (2002) Salvinorin A: A potent naturally occurring nonnitrogenous κ opioid selective agonist. *Proc. Natl. Acad. Sci. U.S.A.* 99, 11934–11939.
- Ansonoff, M. A., Zhang, J., Czyzyk, T., Rothman, R. B., Stewart, J., Xu, H., Zjawiony, J., Siebert, D. J., Yang, F., Roth, B. L., and Pintar, J. E. (2006) Antinociceptive and hypothermic effects of Salvinorin A are abolished in a novel strain of κ -opioid receptor-1 knockout mice. *J. Pharmacol. Exp. Ther.* 318, 641–648.
- Sheffler, D. J., and Roth, B. L. (2003) Salvinorin A: The “magic mint” hallucinogen finds a molecular target in the κ opioid receptor. *Trends Pharmacol. Sci.* 24, 107–109.
- Vortherms, T. A., and Roth, B. L. (2006) Salvinorin A: From natural product to human therapeutics. *Mol. Interventions* 6, 257–265.
- Harding, W. W., Tidgewell, K., Byrd, N., Cobb, H., Dersch, C. M., Butelman, E. R., Rothman, R. B., and Prisinzano, T. E. (2005) Neoclerodane diterpenes as a novel scaffold for μ opioid receptor ligands. *J. Med. Chem.* 48, 4765–4771.
- Harding, W. W., Schmidt, M., Tidgewell, K., Kannan, P., Holden, K. G., Dersch, C. M., Rothman, R. B., and Prisinzano, T. E. (2006) Synthetic studies of neoclerodane diterpenes from *Salvia divinorum*: Selective modification of the furan ring. *Bioorg. Med. Chem. Lett.* 16, 3170–3174.
- Groer, C. E., Tidgewell, K., Moyer, R. A., Harding, W. W., Rothman, R. B., Prisinzano, T. E., and Bohn, L. M. (2007) An opioid agonist that does not induce micro-opioid receptor–arrestin interactions or receptor internalization. *Mol. Pharmacol.* 71, 549–557.
- Simpson, D. S., Katavic, P. L., Lozama, A., Harding, W. W., Parrish, D., Deschamps, J. R., Dersch, C. M., Partilla, J. S., Rothman, R. B., Navarro, H., and Prisinzano, T. E. (2007) Synthetic Studies of Neoclerodane Diterpenes from *Salvia divinorum*: Preparation and Opioid Receptor Activity of Salvinicin Analogues. *J. Med. Chem.* 50, 3596–3603.
- Prisinzano, T. E., and Rothman, R. B. (2008) Salvinorin A analogs as probes in opioid pharmacology. *Chem. Rev.* 108, 1732–1743.
- Yan, F., Mosier, P. D., Westkaemper, R. B., Stewart, J., Zjawiony, J. K., Vortherms, T. A., Sheffler, D. J., and Roth, B. L. (2005) Identification of the molecular mechanisms by which the diterpenoid salvinorin A binds to κ -opioid receptors. *Biochemistry* 44, 8643–8651.
- Vortherms, T. A., Mosier, P. D., Westkaemper, R. B., and Roth, B. L. (2007) Differential helical orientations among related G protein-coupled receptors provide a novel mechanism for selectivity. Studies with salvinorin A and the κ -opioid receptor. *J. Biol. Chem.* 282, 3146–3156.
- Tan, K. R., Gonthier, A., Baur, R., Ernst, M., Goeldner, M., and Sigel, E. (2007) Proximity-accelerated chemical coupling reaction in the benzodiazepine-binding site of γ -aminobutyric acid type A receptors: Superposition of different allosteric modulators. *J. Biol. Chem.* 282, 26316–26325.
- Luo, Y., Knuckley, B., Bhatia, M., Pellechia, P. J., and Thompson, P. R. (2006) Activity-based protein profiling reagents for protein arginine deiminase 4 (PAD4): Synthesis and in vitro evaluation of a fluorescently labeled probe. *J. Am. Chem. Soc.* 128, 14468–14469.
- Cohen, M. S., Zhang, C., Shokat, K. M., and Taunton, J. (2005) Structural bioinformatics-based design of selective, irreversible kinase inhibitors. *Science* 308, 1318–1321.
- Cohen, M. S., Hadjivassiliou, H., and Taunton, J. (2007) A clickable inhibitor reveals context-dependent autoactivation of p90 RSK. *Nat. Chem. Biol.* 3, 156–160.
- Mattras, H., Aliau, S., Demey, E., Poncet, J., and Borgna, J. L. (2006) Mass spectrometry identification of covalent attachment sites of two related estrogenic ligands on human estrogen receptor α . *J. Steroid Biochem. Mol. Biol.* 98, 236–247.

19. Mattras, H., Aliau, S., Richard, E., Bonnafous, J. C., Jouin, P., and Borgna, J. L. (2002) Identification by MALDI-TOF mass spectrometry of 17 α -bromoacetamidopropylestradiol covalent attachment sites on estrogen receptor α . *Biochemistry* 41, 15713–15727.
20. Foucaud, B., Alarcon, K., Sakr, E., and Goeldner, M. (2007) Binding-site chemical probing in homology models using affinity labeling of cysteine-substituted receptors. *Curr. Chem. Biol.* 1, 271–277.
21. Yan, F., Mosier, P. D., Westkaemper, R. B., and Roth, B. L. (2008) G α -Subunits Differentially Alter the Conformation and Agonist Affinity of κ -Opioid Receptors. *Biochemistry* 47, 1567–1578.
22. Xu, W., Chen, C., Huang, P., Li, J., de Riel, J. K., Javitch, J. A., and Liu-Chen, L. Y. (2000) The conserved cysteine 7.38 residue is differentially accessible in the binding-site crevices of the μ , δ , and κ opioid receptors. *Biochemistry* 39, 13904–13915.
23. Xu, W., Campillo, M., Pardo, L., de Riel, J. K., and Liu-Chen, L.-Y. (2005) The Seventh Transmembrane Domains of the δ and κ Opioid Receptors Have Different Accessibility Patterns and Interhelical Interactions. *Biochemistry* 44, 16014–16025.
24. Strachan, R. T., Sheffler, D. J., Willard, B., Kinter, M., Kiselar, J. G., and Roth, B. L. (2009) Ribosomal S6 Kinase 2 Directly Phosphorylates the 5-Hydroxytryptamine 2A (5-HT2A) Serotonin Receptor, Thereby Modulating 5-HT2A Signaling. *J. Biol. Chem.* 284, 5557–5573.
25. Ballesteros, J. A., and Weinstein, H. (1995) Integrated Methods for the Construction of Three-Dimensional Models and Computational Probing of Structure-Function Relations in G Protein-Coupled Receptors. *Methods Neurosci.* 25, 366.
26. Cantescu, A. A., Shelenkov, A. A., and Dunbrack, R. L., Jr. (2003) A Graph-theory Algorithm for Rapid Protein Side-chain Prediction. *Protein Sci.* 12, 2001–2014.
27. Laskowski, R. A., MacArthur, M. W., Moss, D. S., and Thornton, J. M. (1993) PROCHECK: A Program to Check the Stereochemical Quality of Protein Structures. *J. Appl. Crystallogr.* 26, 283–291.
28. Xu, W., Campillo, M., Pardo, L., Kim de Riel, J., and Liu-Chen, L. Y. (2005) The seventh transmembrane domains of the δ and κ opioid receptors have different accessibility patterns and interhelical interactions. *Biochemistry* 44, 16014–16025.
29. Wess, J., Han, S. J., Kim, S. K., Jacobson, K. A., and Li, J. H. (2008) Conformational changes involved in G-protein-coupled-receptor activation. *Trends Pharmacol. Sci.* 29, 616–625.
30. Sansom, M. S., and Weinstein, H. (2000) Hinges, swivels and switches: The role of prolines in signalling via transmembrane α -helices. *Trends Pharmacol. Sci.* 21, 445–451.
31. Edwards, M. D., Li, Y., Kim, S., Miller, S., Bartlett, W., Black, S., Dennison, S., Iscla, I., Blount, P., Bowie, J. U., and Booth, I. R. (2005) Pivotal role of the glycine-rich TM3 helix in gating the MscS mechanosensitive channel. *Nat. Struct. Mol. Biol.* 12, 113–119.
32. Ballesteros, J. A., Jensen, A. D., Liapakis, G., Rasmussen, S. G., Shi, L., Gether, U., and Javitch, J. A. (2001) Activation of the $\beta 2$ -adrenergic receptor involves disruption of an ionic lock between the cytoplasmic ends of transmembrane segments 3 and 6. *J. Biol. Chem.* 276, 29171–29177.
33. Riek, R. P., Finch, A. A., Begg, G. E., and Graham, R. M. (2008) Wide Turn Diversity in Protein Transmembrane Helices Implications for G-Protein-Coupled Receptor and Other Polytopic Membrane Protein Structure and Function. *Mol. Pharmacol.* 73, 1092–1104.
34. Medana, C., Massolini, C., Pazzi, M., and Baiocchi, C. (2006) Determination of salvinorins and divinatorins in *Salvia divinorum* leaves by liquid chromatography/multistage mass spectrometry. *Rapid Commun. Mass Spectrom.* 20, 131–136.
35. Barnes, S., Prasain, J. K., Wang, C. C., and Moore, D. R. II (2006) Applications of LC-MS in the study of the uptake, distribution, metabolism and excretion of bioactive polyphenols from dietary supplements. *Life Sci.* 78, 2054–2059.
36. Ouagazzal, A., Grottick, A. J., Moreau, J., and Higgins, G. A. (2001) Effect of LSD on prepulse inhibition and spontaneous behavior in the rat. A pharmacological analysis and comparison between two rat strains. *Neuropsychopharmacology* 25, 565–575.
37. Geyer, M. A., and Braff, D. L. (1987) Startle habituation and sensorimotor gating in schizophrenia and related animal models. *Schizophr. Bull.* 13, 643–668.
38. Braff, D. L., and Geyer, M. A. (1980) Acute and chronic LSD effects on rat startle: Data supporting an LSD–rat model of schizophrenia. *Biol. Psychiatry* 15, 909–916.
39. Manda, S., Lerner-Marmarosh, N., Hashmi, M., and Abood, L. G. (1992) Opioid receptor antagonist affinity ligands: 6 β -Bromoaceta-mido-6-desoxynaltrexone and 6 β -thioglycolamido-6-desoxynaltrex-one. *Neurochem. Res.* 17, 1191–1194.
40. Tam, S. W., and Liu-Chen, L. Y. (1986) Reversible and irreversible binding of β -funaltrexamine to μ , δ and κ opioid receptors in guinea pig brain membranes. *J. Pharmacol. Exp. Ther.* 239, 351–357.
41. Tam, S. W., Nickolson, V. J., and Liu-Chen, L. Y. (1985) [3 H] β -Funaltrexamine binds covalently to brain opioid receptors. *Eur. J. Pharmacol.* 119, 259–260.
42. Cheng, C. Y., Wu, S. C., Hsin, L. W., and Tam, S. W. (1992) Selective reversible and irreversible ligands for the κ opiate receptor. *J. Med. Chem.* 35, 2243–2247.